

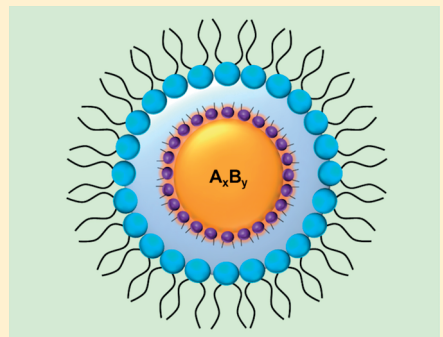
# Reverse Micelles as Templates for the Fabrication of Size-Controlled Nanoparticles: A Physical Chemistry Experiment

C. Harris,\*<sup>id</sup> C. Gaster, and M. C. Gelabert

Department of Chemistry, Physics, and Geology, Winthrop University, Rock Hill, South Carolina 29733, United States

 *Supporting Information*

**ABSTRACT:** Synthesis and characterization of nanomaterials yields opportunities for instruction of related topics in solution chemistry and materials science, as well as spectroscopy connecting to band theory, the *particle in a box* quantum mechanical model, and thermodynamics. In collaboration with an undergraduate research assistant, we have developed a synthesis experiment that investigates the use of reverse micelles as reaction templates for the preparation of size-controlled nanomaterials through simple, controlled precipitation reactions. This experiment is designed for an undergraduate physical or inorganic chemistry laboratory course. The proposed method boasts several advantageous features, including simplicity, functionality both at low temperature and in the presence of oxygen, applicability to a wide variety of compounds including semiconductors and colloidal metals, and precise control of particle size. To demonstrate our method, we chose CdSe as a model system due to its readily observable size-dependent optical effects. The particles produced are well-controlled and show high optical quality. Additionally, the use of reverse micelles allows us to further broaden the scope of this assessment, incorporating other key topics including ligand–metal chelation, nucleation/growth kinetics, thermodynamics, surfactant chemistry, and hydrodynamics.



**KEYWORDS:** *Upper-Division Undergraduate, Physical Chemistry, Inorganic Chemistry, Laboratory Instruction, Hands-On Learning/Manipulatives, Materials Science, Nanotechnology, Micelles, Semiconductors*

## INTRODUCTION

Nanotechnology is a broad field that can be approached from a wide array of perspectives. Nanoparticle synthesis, for example, can introduce students to important, yet routinely overlooked, topics such as surface ligand binding, Ostwald ripening, dangling bonds, and metal ion complexation. These specialized topics can be readily connected to fundamental subjects like thermodynamics and kinetics. Molecular orbital theory, band theory, and other aspects of quantum mechanics can also be addressed through spectroscopic analysis of optical properties.

Some of the more intriguing and educational aspects of nanotechnology are related to the quantum mechanical behavior of semiconductor nanoparticles known as quantum dots, materials exhibiting size-dependent optical properties. Common examples of semiconductor quantum dot materials are metal chalcogenides like CdS, CdSe, ZnS, ZnSe, and PbS. It is straightforward to use nanoparticle electronics to rationalize the *particle in a box* quantum mechanical model. Photoexcitation of a semiconductor leads to the formation of an exciton with a characteristic Bohr radius. If the nanoparticle radius is reduced below the Bohr radius, the exciton is confined and in this way can be envisioned as a particle in a box.<sup>1</sup> Further, as the particle size continues to decrease, the energy required to generate the exciton increases, leading to a blue shift of the absorbance, characterized by sharp color changes in the material from “more red” to “more blue”.

Several experiments and teaching tools for chemistry courses related to quantum dot phenomena have been reported in this *Journal*,<sup>1–8</sup> and some authors have applied these properties to the fabrication of photovoltaic devices.<sup>4</sup> CdSe, in particular, has drawn significant attention because of its favorable optoelectronic parameters, which include a low band gap, a strong molar absorptivity, and a relatively large Bohr radius.<sup>2</sup> These parameters enable straightforward observation of quantum mechanical behavior in CdSe, as this material can be theoretically tuned to vary in color across the entire span of the visible spectrum. This is not only informative to the students, but also visually appealing. A common synthetic method for the synthesis of well-controlled CdSe quantum dots adopted into undergraduate laboratories is the reaction of CdO and Se in octadecene and trioctyl phosphine at an elevated temperature of 225 °C (TOPO method).<sup>3</sup> Another report, comparing quantum dots to organic dyes, uses commercially available CdSe nanoparticles.<sup>9</sup> However, synthetic methods of *monodisperse, well-controlled* CdSe nanoparticles, at low temperatures with air-stable reagents, for adoption into undergraduate laboratory experiments are relatively lacking.

**Received:** August 9, 2018

**Revised:** December 20, 2018

Here, we report a simple, low-temperature, ambient atmosphere method for the synthesis of monodisperse CdSe nanoparticles with precisely tunable sizes using water-in-oil reverse micelles as nanoscale templates for particle growth. This experiment, developed at Winthrop over several years, produces particles of optical quality nearly equivalent to that for particles from established synthetic methods of CdSe fabrication that are generally more complex, costly, and hazardous. Although CdSe has been selected as a prototypical system, the proposed method can readily be modified to prepare many other types of compounds. Additionally, the use of reverse micelles enables a broader scope, incorporating specialized topics including surfactant chemistry and hydrodynamics.

### Reverse Micelles

The employed synthetic method utilizes the anionic surfactant sodium dioctylsulfosuccinate, commonly referred to as Aerosol-OT (AOT). The structure is composed of a bulky sulfonate “head” group and a split 8-carbon “tail”. To a highly concentrated solution of AOT in heptane, a small volume of water is added. Upon mixing, strong hydrogen bonds are formed between the water and the head group, and reverse micelles are formed, with aqueous cores stabilized by surfactant molecules within a nonpolar solvent (Figure 1).<sup>10</sup> Due to the

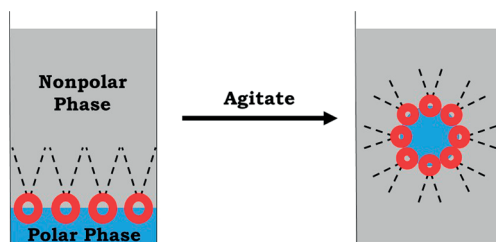


**Figure 1.** Depiction of reverse micelle formation. Circles represent the surfactant head groups, while dashed lines represent the nonpolar tail groups which extend outward into the nonpolar phase.

parameters of AOT (i.e., head volume tail length cross-sectional area), reverse micelles formed by AOT are spherical, ideal for exhibiting three-dimensional confinement effects. Surfactants with very long tail lengths, such as cetyltrimethylammonium bromide, will produce more cylindrical structures. The spherical shape of the water pool minimizes the interfacial surface area between the water and the nonpolar phase, ensuring that a majority of water molecules are stabilized within the core of the pool. The length and conical shape of the tail groups facilitate a high degree of interaction with straight-chain solvents like heptane, allowing for very high AOT solubility in the solvent and forcing the surfactant-bound water droplets to disperse uniformly (Figure 1, right). Because of their small size, reverse micelles are subject to Brownian motion.<sup>11</sup> Constant collisions between micelles and spontaneous exchange of solutes result in a Poisson distribution of solutes throughout micellar dispersions.<sup>11,12</sup> As a result of these exchange processes, size-limited precipitates can be synthesized via simple precipitation or redox reactions that occur inside the reverse micelles.<sup>11,13–15</sup> Since our precursors are ionic and highly water-soluble, they are readily dispersed within the confines of the reverse micelles, essentially utilizing the micelles as templates to restrict the particle size and shape, as described in Figure 2.

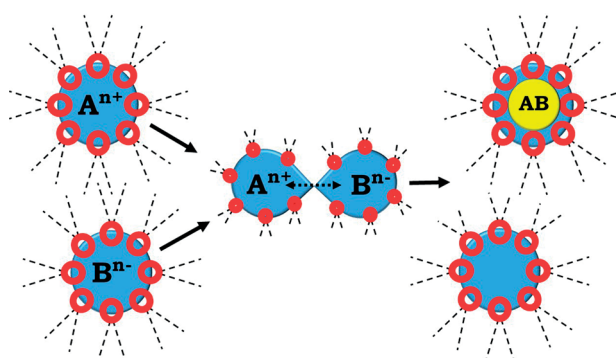


**Figure 2.** Formation of size-limited precipitates initiated by collisions between precursor-loaded reverse micelles.

The size of the aqueous core of the micelle, referred to as a “water pool”, is dictated by the ratio of the concentrations of water to AOT in the nonpolar solvent:<sup>13</sup>

$$\frac{r^3}{(r - L)^3} = 1 + \frac{V_2}{w_o V_1} \quad (1)$$

In this equation,  $r$  is the water pool radius,  $L$  is the estimated length of the AOT tail group (15 Å),  $V_1$  is the estimated volume of a water molecule (30 Å<sup>3</sup>),  $V_2$  is the estimated volume of an AOT molecule (825 Å<sup>3</sup>), and  $w_o$  is the concentration ratio [H<sub>2</sub>O]/[AOT]. The inherent instability of nanoparticles results from large differences in potential energy between surface and core atoms. While atoms within the core of a particle are fully saturated, atoms on the surface are unsaturated and, thus, are higher in potential energy. The system conditions are thermodynamically favorable for Ostwald ripening, an exothermic process where smaller particles tend to merge into larger particles to minimize the fraction of surface atoms. Even within the boundaries of a reverse micelle, the randomness of this process produces wide variations in particle size. However, if a sufficient concentration of ligand is present in the water pool, the binding of the ligand to the particle surface (passivation) can compete kinetically with Ostwald ripening to enable the stabilization of nanosized particles, if the change in enthalpy from particle/ligand interaction exceeds that of the particle/particle interaction. Passivation also narrows the particle size distribution, thus enabling more monodisperse products. Thiolates are excellent ligands for this study due to their exceptionally high binding affinity for terminal Cd atoms, and L-cysteine was chosen as the ligand. These points are discussed further in the **Experimental Section**, as well as our evaluation of size uniformity.

As described, this synthetic approach simply consists of the following: (1) confined media which serve as a template for particle formation, (2) complexed precursor ions, and (3) a surface-binding ligand. This method is applicable to virtually any binary semiconductor that can be produced via a low-temperature precipitation reaction in aqueous solution, although it is up to the instructor to select appropriate reagents, ligands, and complexing agents for the material being synthesized. This is a beneficial feature, particularly for institutions with strict guidelines regarding the use of toxic heavy metals such as cadmium. The reaction mechanism is described in further detail in a later section.

**Table 1. Suggested Parameters for Synthesis of Size-Controlled CdSe Nanoparticles in Reverse Micelles**

Volumes of Components of Ligand Micelle Solution, mL <sup>a</sup>			Volumes of Components of Cd <sup>2+</sup> /SeSO <sub>3</sub> <sup>2-</sup> Micelle Solution, mL <sup>a,b,c</sup>				After Mixing					
AOT(hep)	Cys <sup>2-</sup> (aq)	H <sub>2</sub> O	AOT(hep)	Cd <sup>2+</sup> (aq)	SeSO <sub>3</sub> <sup>2-</sup> (aq)	H <sub>2</sub> O	[Lig]/[Cd <sup>2+</sup> ]	w <sub>o</sub>	Pool Diam, nm	λ <sub>onset</sub> <sup>d</sup> , nm	Particle Diam, nm <sup>e</sup>	Color
3.00	0.40	0.00	3.00	0.12	0.10	0.18	3.33	14.8	10.2	444	3.54	Green
3.00	0.25	0.15	3.00	0.12	0.10	0.18	2.08			479	3.92	Yellow
3.00	0.20	0.20	3.00	0.12	0.10	0.18	1.67			500	4.16	Dark yellow
3.00	0.15	0.25	3.00	0.12	0.10	0.18	1.25			534	4.66	Orange

<sup>a</sup>The total volumes of polar and nonpolar media in each micelle solution are held constant at 0.400 and 3.00 mL, respectively, for a fixed  $w_o$  value of 14.8. <sup>b</sup>The Cd:Se ratio is fixed at 1.2:1. <sup>c</sup>The selenosulfate precursor acts as the limiting reactant. <sup>d</sup>Onset absorbance wavelengths are obtained from extrapolation of the absorbance spectra in Figure 3. <sup>e</sup>Particle sizes are dependent on the [ligand]/[metal] ratio.

## EXPERIMENTAL SECTION

This experiment was developed for the Physical Chemistry II laboratory course, included in the curriculum since 2015. Lab students are concurrently enrolled in the companion lecture course covering quantum mechanics and spectroscopy. Including the prelaboratory lecture, the experiment requires approximately 3 h to complete. The average enrollment of the lab sections is approximately 12 students, split into several groups of 2 for this work. The experiment is completed in a single weekly session.

Reagents were used as received: sodium dioctylsulfosuccinate (96%), cadmium chloride anhydrous (laboratory grade), ammonium thiocyanate (98%+), ammonium hydroxide solution (ACS grade), selenium powder (99.5%), sodium sulfite (98%+), hydrazine hydrate (98%+), potassium hydroxide (ACS grade), and L-cysteine (98%+). It is recommended that the course instructor or laboratory support staff prepare the stock solutions in advance of the class. Detailed instructions for solution preparation, student handout, and other laboratory logistics are available in the [Supporting Information](#) files.

The surfactant solution is 0.5 M AOT in heptane (nonpolar phase). The selenide source is 0.1 M SeSO<sub>3</sub><sup>2-</sup>(aq), maintained at 70 °C. The cadmium source is a stable, pH-resistant Cd<sup>2+</sup>(aq) complex, 0.1 M Cd(SCN)<sub>2</sub>(NH<sub>3</sub>)<sub>2</sub>(aq). The ligand solution is 0.1 M cysteine(aq). The pH of the ligand solution is adjusted to ~13 with base, and hydrazine is added to minimize S–S cross-linking. In the laboratory, all of these solutions, as well as neat heptane, are placed in a fume hood. Micropipettes, ultrasonic baths, and capped 20 mL vials are placed throughout the laboratory.

### Micellar Reaction

The preparation of each particle solution requires the combination of two separate micellar solutions: the ligand/micelle solution and the cadmium/selenosulfate/micelle solution (Table 1). Typically, each member of the group assumes responsibility of preparing one of these solutions. The first solution is prepared by adding specific volumes of the aqueous cysteine solution and water to a vial containing 3 mL of 0.5 M AOT in heptane. The resulting mixture will initially appear cloudy, and then become *totally* transparent as the micelles homogenize and distribute throughout the nonpolar phase following 2–3 min of sonication. Afterward, this solution is set aside and stirred with a magnetic stir bar.

The second micelle solution contains *both* the Cd<sup>2+</sup>(aq) and SeSO<sub>3</sub><sup>2-</sup>(aq) precursors. Specific volumes of the Cd<sup>2+</sup> stock solution and any additional neat water are added to 3 mL of the surfactant solution and sonicated to transparency. Then,

the required volume of the SeSO<sub>3</sub><sup>2-</sup> stock is added, and the solution is sonicated again to transparency. The Cd<sup>2+</sup>/Se<sup>2-</sup> ratio is maintained at 1.20:1. The selenosulfate precursor should be added last due to its thermal instability, and the resulting mixture should be used within 5 min of sonication.

The second solution is added to the first, slowly and dropwise with rapid stirring, over a period of 2–3 min to initiate particle formation. The particle solutions are allowed ~10 min to age, during which time the students begin preparing their next particle solution.

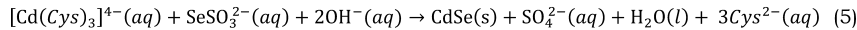
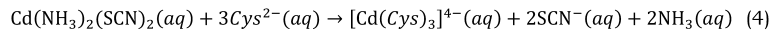
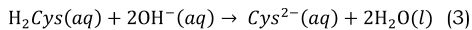
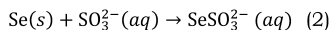
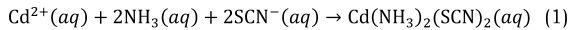
### UV-Vis Spectrophotometry

To collect spectral data, the students added aliquots of their particle solutions into glass cuvettes, diluting with neat heptane in a 1:4 ratio. The cuvettes were loaded into a Jasco V-660 spectrophotometer, and the solutions were scanned in the range 700–400 nm. Students exported their data in Excel format. For a standard 3 h laboratory course, students have time to prepare and analyze 2–3 particle solutions. Although we did not include fluorescence analysis in our practicum, such analysis may easily be incorporated into this experiment. For a *qualitative* analysis, simple UV lamps with lightbox can be used, and the students can simply report on the observed emission and rationalize their observation on the basis of the optical properties of their particles. For a more *quantitative* analysis, the emission spectra of the solutions can be obtained with fluorimetry. If the emission and absorbance spectra are plotted together on the same graph versus wavelength, the students can calculate and rationalize the observed Stokes shift on the basis of their knowledge of band structure and relaxation modes.

## HAZARDS AND SAFETY PRECAUTIONS

All procedures should be done with appropriate safety apparel and best practices for eye, skin, and lung protection. Cadmium chloride, elemental selenium, and hydrazine are acutely toxic, and hydrazine poses additional fire and corrosive hazards. Heptane poses health, fire, and environmental hazards, and potassium hydroxide and sodium dioctylsulfosuccinate (AOT) are corrosion and health hazards. All chemicals used in this experiment pose additional environmental or aquatic hazards, except L-cysteine and sodium sulfite, which pose no significant hazards but, as for any chemical, should be treated with care.

Reflux synthesis of the selenosulfate anion, SeSO<sub>3</sub><sup>2-</sup>, is best done in a fume hood, and all stock chemicals should be maintained in a fume hood until ready for use. Micropipettes and tightly sealed vials for the sonicating bath are used throughout the experiment to avoid exposure to vapors. Qualitative observations of solution emission with an ultra-

**Scheme 1. Proposed Reaction Mechanism**

violet lamp should be done only with closed vials, and for UV-vis spectroscopy, glass or quartz cuvettes with tight lids should be used.

**RESULTS AND DISCUSSION****Mechanism**

The proposed reaction scheme mechanism is as shown in Scheme 1.

The initial step in this reaction scheme, step 1, is the formation of a sterically hindered, tetrahedral  $\text{Cd}^{2+}$  complex.<sup>16</sup> This complex will not readily react with selenosulfate, allowing precursors to be coupled within the same water pools for improved reproducibility. Additionally, the  $\text{Cd}^{2+}$  ion is protected against formation of the insoluble hydroxide,  $\text{Cd}(\text{OH})_2$ , a very important consideration due to the basic pH of both the selenosulfate (pH 8) and ligand solutions (pH > 13). The  $\text{SeSO}_3^{2-}$  anion, structurally similar to sulfate, but with an oxygen atom substituted by a selenium atom, forms by oxidation of sulfite, as described in step 2. When the  $\text{Cd}^{2+}/\text{SeSO}_3^{2-}$  solution is added to the ligand solution, strong attractive interactions between  $\text{Cd}^{2+}$  and deprotonated cysteine molecules lead to the dissociation of the tetrahedral complex in step 1 and the formation of a trigonal complex,  $\text{Cd}(\text{Cys})_3^{4-}$ , as shown in step 4<sup>17</sup> which is *not* sterically hindered. This new complex is then immediately attacked by selenosulfate to yield  $\text{CdSe}$  in step 5. An excess of  $\text{Cd}^{2+}$  is used to ensure a mostly  $\text{Cd}$ -terminated particle surface. The high local concentration of the free thiolate ligand and unusually high binding affinity of the thiolate for the  $\text{Cd}$ -terminated particle surface<sup>18</sup> drive rapid kinetics for attachment of the ligand to the  $\text{CdSe}$  surface, competing with particle aggregation and allowing for control of the particle diameter.

**Analysis of Spectral Data**

At a fixed  $[\text{Cd}^{2+}]/[\text{Se}^{2-}]$  ratio, the particle size is dictated primarily by the  $[\text{ligand}]/[\text{Cd}^{2+}]$  ratio. Because the total volume of water is unchanged, the water pool size is fixed. This is depicted by the absorbance spectra shown in Figure 3. Increasing the amount of ligand results in significant blue-shifting of the onset of absorbance. The extent of the blue shift is maximized at a  $[\text{ligand}]/[\text{Cd}^{2+}]$  ratio of approximately 3.33. Further addition of ligand has a negligible effect on the onset absorbance, suggesting a lower limit of particle size based on the parameters of this particular method. The claim of a narrow particle size distribution for each solution is based on comparison of the band widths to those observed for  $\text{CdSe}$  nanoparticles prepared using the TOPO method, which is widely regarded as the most precise wet method of producing size-controlled particles.<sup>19</sup> The UV-vis absorbance spectra of high-quality  $\text{CdSe}$  quantum dots are well-known to display distinct peaks. The wavelength corresponding to a given peak is size-dependent when the particle is quantized ( $d < 11.2 \text{ nm}$ ). When a large range of particle sizes exists in a solution, the

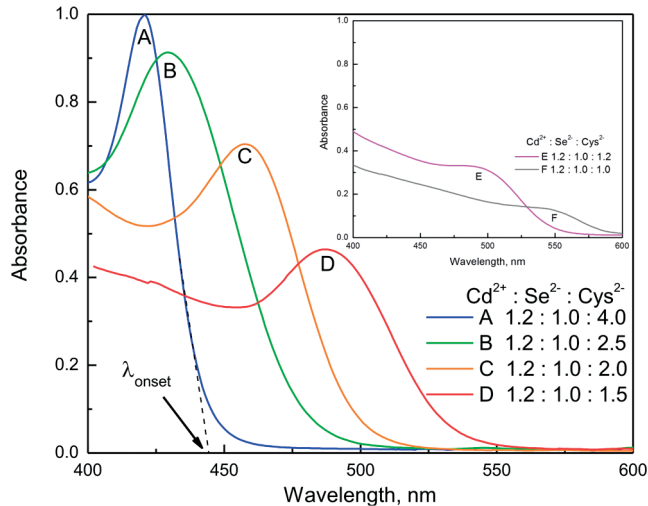


**Figure 3.** Normalized absorbance spectra. The reference solution is a uniform micellar solution made from 3.00 mL of [AOT] and 0.400 mL of deionized water. The value of  $\lambda_{\text{onset}}$  is estimated by extrapolation of the spectral trace to the  $x$ -axis, as shown above. The inset trace shows the loss of spectral resolution as the ligand concentration decreases below the critical value.

individual spectral traces corresponding to the various particle sizes will sum together to produce a broad “spectral shoulder” as described by Figure 3. Thus, the band width is directly related to the degree of monodispersivity.<sup>20</sup>

At a  $[\text{ligand}]/[\text{Cd}^{2+}]$  ratio of less than 1.25, the particle size distribution becomes large. This is made evident by the complete loss of a discernible absorbance peak and substantial broadening of the spectral trace (Figure 3 inset). The colors of the solutions having suitable optical quality range from green to orange. The estimated diameters of the particles shown in Table 1 are calculated from Brus’ equation (eq 2), which relates the size of a particle to the energy of its lowest excited state.

$$\Delta E_g = \frac{h^2}{8R^2} \left( \frac{1}{m_e^*} + \frac{1}{m_h^*} \right) - \frac{1.8e^2}{4\pi\epsilon\epsilon_0 R} \quad (2)$$

In this equation,  $\Delta E_g$  is the energetic extent of the blue shift from the bulk state, determined using onset wavelengths rather than peak wavelengths because they are more representative of the lowest-energy transition. The onset energies are determined by extrapolating the linear portion of the absorbance peak to the wavelength axis.  $R$  is the particle radius, and  $h$  is Planck’s constant.  $m_e^*$  and  $m_h^*$  are the effective electron and hole masses of  $\text{CdSe}$  ( $0.13m_e$  and  $0.45m_e$ , respectively<sup>18</sup>), where  $m_e$  is the rest mass of an electron,  $e$  is the charge of an electron,  $\epsilon_0$  is the permittivity of vacuum ( $8.854 \times 10^{-12} \text{ m}^{-3} \text{ kg}^{-1} \text{ s}^4 \text{ A}^2$ ), and  $\epsilon$  is the unitless dielectric constant of the  $\text{CdSe}$ . Although the dielectric constant of  $\text{CdSe}$  is

known to exhibit size dependence,<sup>21</sup> it is simple and convenient to use the value corresponding to the bulk state,  $\epsilon = 10.6$ .<sup>1,22,23</sup>

## ■ TEACHING OBJECTIVES

This project is intended to provide students with an insight into the key facets of synthetic methods and spectroscopic behavior of nanoparticles, while also introducing them to a wide array of correlated concepts spanning both classical and quantum mechanics. The incorporation of reverse micelles builds upon the students' knowledge of surfactants, intermolecular forces, and thermodynamics from their general chemistry curricula while providing a practical application of familiar concepts. A simplified explanation of the thermodynamics of particle growth is also provided by this experiment. The concepts of Ostwald ripening and surface ligands are introduced to students for the first time, and the kinetic competition between Ostwald ripening and ligand binding is clearly depicted as a key factor in controlling the size distribution of nanoparticles. Furthermore, the students learn about the significance of ion complexes in solution chemistry and their immense usefulness in slowing reaction kinetics to allow greater precision in controlling particle size. Finally, spectroscopic analysis of the size-dependent optical properties of the resulting particles provides confirmation of the "particle in a box" model, further emphasizing its applicability to specific physical systems, and therefore its importance beyond introductory quantum mechanics.

## ■ CONCLUSION

This experiment has provided a simple, yet advanced, synthesis that students could perform collaboratively. The resulting solutions are visually stimulating, and the spectroscopic data obtained provide a wealth of information. Laboratory reports were used to assess student learning outcomes. In these formal assignments, the students demonstrated a strong understanding of the synthetic process. They were asked to discuss the roles of the components (i.e., micelles, ligands, complexing agents) and parameters (i.e.,  $w_o$ , Cd/Se ratio, ligand/Cd ratio) of the experiment and justify the appearances of their products on the basis of changes to the parameters, as well as to think critically to predict how further manipulation of the system would affect products. Additionally, students were able to successfully use their spectroscopic data to solve Brus' equation to determine particle sizes, from which they also calculated agglomeration numbers and particle molarities. At the conclusion of this experiment, the students possessed a much deeper understanding of nanoscale materials science and were able to better recognize the *real world* correlation of the "particle in a box" theoretical model to experimental observations.

## ■ ASSOCIATED CONTENT

### § Supporting Information

The Supporting Information is available on the ACS Publications website at DOI: [10.1021/acs.jchemed.8b00630](https://doi.org/10.1021/acs.jchemed.8b00630).

Notes for instructors ([PDF](#), [DOCX](#))

Student handout and prelaboratory and postlaboratory assignments ([PDF](#), [DOCX](#))

## ■ AUTHOR INFORMATION

### Corresponding Author

\*E-mail: [harrisc@winthrop.edu](mailto:harrisc@winthrop.edu).

### ORCID

C. Harris: 0000-0003-1263-7597

### Notes

The authors declare no competing financial interest.

## ■ ACKNOWLEDGMENTS

The authors would like to thank the Department of Chemistry, Physics, and Geology, Winthrop University, SC-EPSCoR #17-RE06 and MADE in SC NSF #1655740 for financial support of this project.

## ■ REFERENCES

- (1) Kippeny, T.; Swafford, L. A.; Rosenthal, S. J. Semiconductor Nanocrystals: A Powerful Visual Aid for Introducing the Particle in a Box. *J. Chem. Educ.* **2002**, *79* (9), 1094.
- (2) Meulenberg, R. W.; Lee, J. R. I.; Wolcott, A.; Zhang, J. Z.; Terminello, L. J.; van Buuren, T. Determination of the Exciton Binding Energy in CdSe Quantum Dots. *ACS Nano* **2009**, *3* (2), 325–330.
- (3) Nordell, K. J.; Boatman, E. M.; Lisenky, G. C. A Safer, Easier, Faster Synthesis for CdSe Quantum Dot Nanocrystals. *J. Chem. Educ.* **2005**, *82* (11), 1697.
- (4) Bauer, C. A.; Hamada, T. Y.; Kim, H.; Johnson, M. R.; Voegtle, M. J.; Emrick, M. S. An Integrated, Multipart Experiment: Synthesis, Characterization, and Application of CdS and CdSe Quantum Dots as Sensitizers in Solar Cells. *J. Chem. Educ.* **2018**, *95* (7), 1179–1186.
- (5) Landry, M. L.; Morrell, T. E.; Karagounis, T. K.; Hsia, C.-H.; Wang, C.-Y. Simple Syntheses of CdSe Quantum Dots. *J. Chem. Educ.* **2014**, *91* (2), 274–279.
- (6) Rice, C. V.; Giffin, G. A. Quantum Dots in a Polymer Composite: A Convenient Particle-in-a-Box Laboratory Experiment. *J. Chem. Educ.* **2008**, *85* (6), 842.
- (7) Winkler, L. D.; Arceo, J. F.; Hughes, W. C.; DeGraff, B. A.; Augustine, B. H. Quantum Dots: An Experiment for Physical or Materials Chemistry. *J. Chem. Educ.* **2005**, *82* (11), 1700.
- (8) Shekhirev, M.; Goza, J.; Teeter, J. D.; Lipatov, A.; Sinitskii, A. Synthesis of Cesium Lead Halide Perovskite Quantum Dots. *J. Chem. Educ.* **2017**, *94* (8), 1150–1156.
- (9) Hutchins, B. M.; Morgan, T. T.; Ucak-Astarlioglu, M. G.; Williams, M. E. Optical Properties of Fluorescent Mixtures: Comparing Quantum Dots to Organic Dyes. *J. Chem. Educ.* **2007**, *84* (8), 1301.
- (10) Maitra, A. Determination of Size Parameters of Water-Aerosol OT-Oil Reverse Micelles from Their Nuclear Magnetic Resonance Data. *J. Phys. Chem.* **1984**, *88* (21), 5122–5125.
- (11) Fletcher, P. D. I.; Robinson, B. H.; Tabony, J. A Quasi-Elastic Neutron Scattering Study of Water-in-Oil Microemulsions Stabilised by Aerosol-OT. Effect of Additives Including Solubilised Protein on Molecular Motions. *J. Chem. Soc., Faraday Trans. 1* **1986**, *82* (8), 2311–2321.
- (12) Pileni, M. P. Reverse Micelles as Microreactors. *J. Phys. Chem.* **1993**, *97* (27), 6961–6973.
- (13) Infelta, P. P.; Gratzel, M.; Thomas, J. K. Luminescence Decay of Hydrophobic Molecules Solubilized in Aqueous Micellar Systems. Kinetic Model. *J. Phys. Chem.* **1974**, *78* (2), 190–195.
- (14) Sant, P. A.; Kamat, P. V. Interparticle Electron Transfer between Size-Quantized CdS and TiO<sub>2</sub> Semiconductor Nanoclusters. *Phys. Chem. Chem. Phys.* **2002**, *4* (2), 198–203.
- (15) Harris, C.; Kamat, P. V. Photocatalysis with CdSe Nanoparticles in Confined Media: Mapping Charge Transfer Events in the Subpicosecond to Second Timescales. *ACS Nano* **2009**, *3* (3), 682–690.

(16) Banerjee, S.; Wu, B.; Lassahn, P.-G.; Janiak, C.; Ghosh, A. Synthesis, Structure and Bonding of Cadmium(II) Thiocyanate Systems Featuring Nitrogen Based Ligands of Different Denticity. *Inorg. Chim. Acta* **2005**, *358* (3), 535–544.

(17) Jalilehvand, F.; Leung, B. O.; Mah, V. Cadmium(II) Complex Formation with Cysteine and Penicillamine. *Inorg. Chem.* **2009**, *48* (13), 5758–5771.

(18) Knauf, R. R.; Lennox, J. C.; Dempsey, J. L. Quantifying Ligand Exchange Reactions at CdSe Nanocrystal Surfaces. *Chem. Mater.* **2016**, *28* (13), 4762–4770.

(19) Peng, Z. A.; Peng, X. Formation of High-Quality CdTe, CdSe, and CdS Nanocrystals Using CdO as Precursor. *J. Am. Chem. Soc.* **2001**, *123* (1), 183–184.

(20) Pesika, N. S.; Stebe, K. J.; Searson, P. C. Relationship between Absorbance Spectra and Particle Size Distributions for Quantum-Sized Nanocrystals. *J. Phys. Chem. B* **2003**, *107* (38), 10412–10415.

(21) Weng, C.-L.; Chen, I.-C.; Tsai, Y.-C. Electron–Acoustic-Phonon Interaction in Core/Shell Nanocrystals and in Quantum-Dot Quantum Wells. *Phys. Rev. B: Condens. Matter Mater. Phys.* **2007**, *76* (19), 195313.

(22) Rabani, E.; Hetényi, B.; Berne, B. J.; Brus, L. E. Electronic Properties of CdSe Nanocrystals in the Absence and Presence of a Dielectric Medium. *J. Chem. Phys.* **1999**, *110* (11), 5355–5369.

(23) Efros, A. L.; Rosen, M.; Kuno, M.; Nirmal, M.; Norris, D. J.; Bawendi, M. Band-Edge Exciton in Quantum Dots of Semiconductors with a Degenerate Valence Band: Dark and Bright Exciton States. *Phys. Rev. B: Condens. Matter Mater. Phys.* **1996**, *54* (7), 4843–4856.